Mediated alkaline flow batteries: from fundamentals to application

Teresa Páez,[a] Alberto Martínez-Cuezva,[b] Jesús Palma,[a] and Edgar Ventosa[a]*

a) IMDEA Energy, Avda. Ramón de la Sagra 3, E-28935 Móstoles, Madrid, Spain

b) Departamento de Química Orgánica, Facultad de Química, Regional Campus of International Excellence "Campus Mare Nostrum", Universidad de Murcia, E-30100, Murcia, Spain

KEYWORDS energy storage; batteries; redox mediators; energy density; ferrocyanide

ABSTRACT: Alkaline flow batteries are attracting increasing attention for stationary energy storage. Very promising candidates have been proposed as active species for the negative compartment, while potassium ferrocyanide ($K_4Fe(CN)_6$) has been the only choice for the positive one. The energy density of this family of batteries is limited by the low solubility of $K_4Fe(CN)_6$ in alkaline media. Herein, we propose a general strategy to increase the energy density of this family of alkaline flow batteries by storing energy in commercial $Ni(OH)_2$ electrodes confined in the positive reservoir. In this way, $K_4Fe(CN)_6$ dissolved in the electrolyte acts not only as electroactive species, but also as charge carrier between current collector and solid $Ni(OH)_2$ particles located in an external reservoir. A storage capacities of 29 Ah L^{-1} for the positive compartment is demonstrated. The concept is implemented in three systems: Zn – $K_4Fe(CN)_6$, anthraquinone – $K_4Fe(CN)_6$ and phenazine – $K_4Fe(CN)_6$ alkaline flow battery, showing the versatility of the strategy. Challenges and future directions to exceed the 16 Wh L_{total}^{-1} demonstrated in this work are discussed.

INTRODUCTION

Energy storage technologies have become of vital importance for a variety of applications ranging from integration of intermittent renewable energy sources in the electrical grid to portable electronics. For stationary energy storage applications, redox flow batteries (RFB) are especially suitable due to their long cycle life and the independent scalability of energy and power (**Figure 1a**).[1,2,3] In a RFB, electrical energy is stored as chemical energy in the electroactive species that are dissolved in the electrolyte. The state-of-art RFB is the all-vanadium redox flow battery (AVRFB), which employs redox electrolytes consisting in vanadium species dissolved in strong acidic media.[4] Electrochemical performances of AVRFBs are competitive for stationary applications; however, vanadium is considered to be a strategic/critical material for the US government[5] as well as the EU commission.[6] In addition, the corrosive vanadium electrolytes are not environmentally friendly. Therefore, finding alternative chemistries for redox flow batteries has become of tremendous interest. Electroactive species based on organic molecules and non-critical elements in alkaline media have attracted much attention in recent years. Several battery chemistries have been demonstrated to deliver promising performances including anthraquinone – $K_4Fe(CN)_6$,[2] vitamin B- derivatives – $K_4Fe(CN)_6$,[7] alloxazine – $K_4Fe(CN)_6$,[8] phenazine-derivatives – $K_4Fe(CN)_6$.[9] All these systems use potassium ferrocyanide (a food additive)[10] as active species in the positive compartment. Unfortunately, the solubility of ferrocyanide-ion decreases with increasing pH, becoming relatively low in alkaline media (ca. 0.4 mol L^{-1} in in 1 M KOH) and limiting its volumetric charge storage capacity to ca. 10 Ah L^{-1}. As a result, the energy density of all these alkaline flow batteries is currently limited by low charge storage capacity of ferrocyanide since the volume of the positive reservoir needs to be from 4-fold to 10-fold larger than that of the negative reservoir (**Figure 1b**). While progress in this direction was recently achieved in neutral pH,[11] efforts should be devoted for improving volumetric charge storage capacities of the positive compartment in alkaline media.

On the other hand, volumetric charge storage capacity of solid battery materials is much higher than that of redox electrolytes, e.g. 1180 Ah L^{-1} for bulk $Ni(OH)_2$ solid particles versus 10 Ah L^{-1} of a ferrocyanide solution. However, solid active materials cannot be used in flow batteries since electrical contact between the electrode located in the electrochemical reactor and the active solid material located in the external reservoir is required. The electrochemical reactor and the external reservoir are tens of centimeters or even meters apart from each other, which prevents charge storage in active solid materials located in the external reservoir. Recently, Wang´s group showed that a redox electrolyte consisting of one single electroactive species can act as charge mediator so that charge can be stored in solid active materials located in the external reservoir of a flow battery.[12,13]

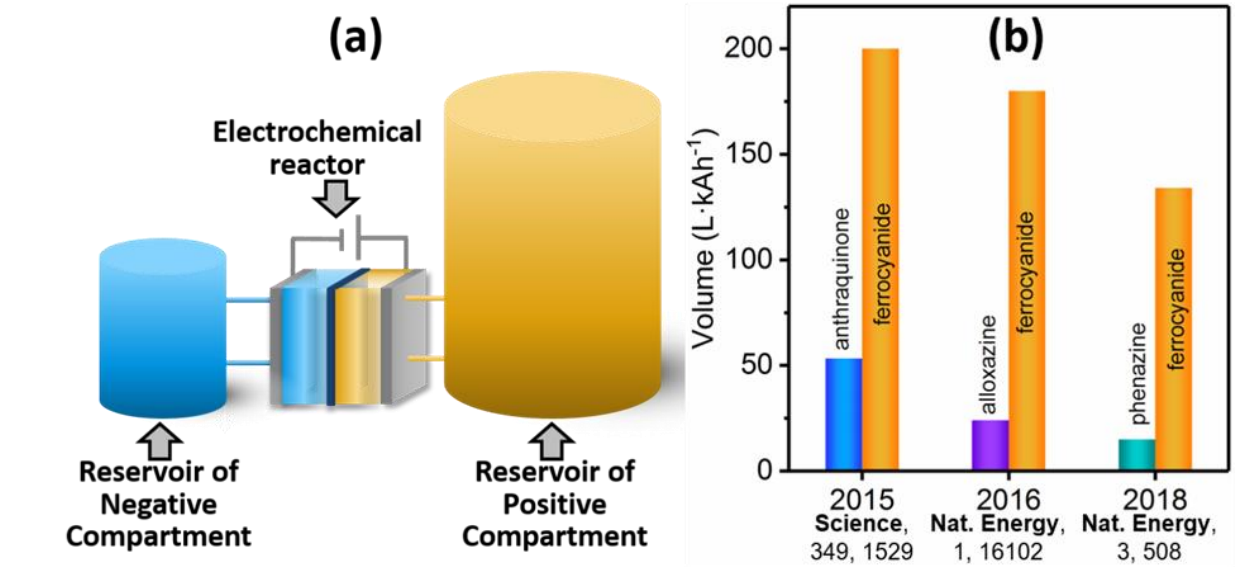

Figure 1. (**a**) Schematic illustration of an alkaline redox flow battery and (**b**) volume of redox electrolyte required to store 1 kAh for three of the most promising flow systems.[2,8,9]

Herein, we present a general strategy to increase the volumetric charge storage capacity of the positive compartment and, thus, the energy density of the rich family of ferrocynide-based alkaline flow batteries. We propose the use of commercial $Ni(OH)_2$ electrodes as solid electroactive material confined in the external reservoir since the volumetric charge storage capacity of $Ni(OH)_2$ is two order of magnitude higher than the maximum value of a ferrocyanide solution. In this way, the pair ferrocyanide - ferricyanide acts not only as electroactive species to store charge, but also as charge mediator between the electrode and solid $Ni(OH)_2$ particles located in an external reservoir.

RESULTS

Concept and Thermodynamics of Charge Transfer Reaction between Electrolyte – Solid. In a flow battery, electroactive species are, by definition, stored in external reservoirs while the charge transfer reaction occurs in the electrochemical reactor so that energy (size of the reservoirs) and power (size of the electrochemical reactor) are decoupled. Thus, electroactive species are dissolved in the electrolyte so that these species can travel from the reservoir where they are stored to the electrochemical reactor where charge is transferred, and vice versa. Energy density is thus limited by the solubility of the dissolved redox species. To overcome this limitation, we propose a family of alkaline flow battery in which dissolved active species in the limiting compartment (ferricyanide/ferrocyanide) not only store energy, but also act as mediator to enable reversible charge storage in high-energy solid active materials confided in the reservoir (**Figure 2**). As a result, the presence of a high-energy solid material in the positive reservoir would allow the size of this reservoir to be significantly reduced, leading to an increase in energy density of the system.

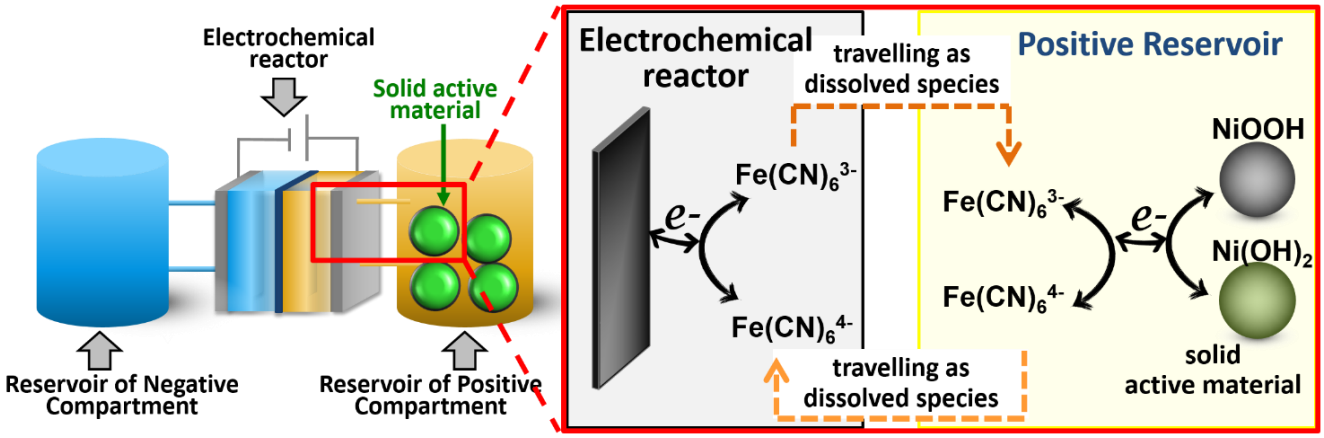

Figure 2. Schematic illustration of the concept of mediated alkaline flow battery in which dissolved active species in the limiting compartment (ferricyanide/ferrocyanide) not only store energy, but also act as charge mediator to enable reversible charge storage in high-energy solid active materials confined in the reservoir.

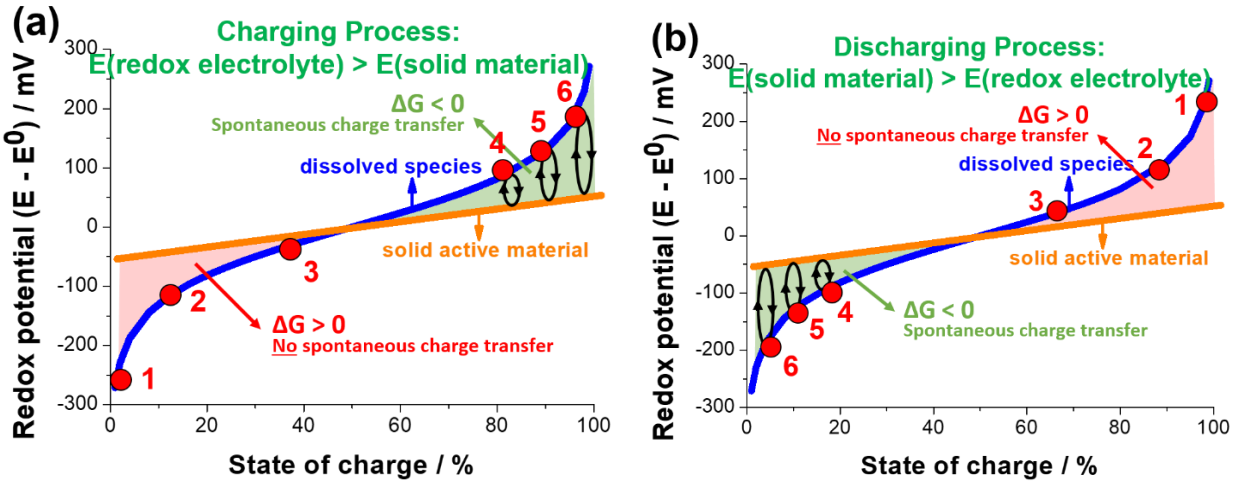

Figure 3. Schematic illustration of the evolution of redox potential with state of charge for dissolved species and solid active material. When ΔG < 0 (green area), spontaneous charge transfer reaction can thermodynamically occur between dissolved species and solid active material. Example for a positive electrode during (a) charging and (b) discharging process.

Spontaneous charge transfer reaction between redox electrolyte and solid active material needs to be reversible which is thermodynamically possible under specific conditions (**Figure 3**). Fundaments of this figure and the reversibility of charge transfer reaction are found in Supporting Information (Section 1 in ESI). In brief, the potential of the reduction reaction must be above that of the oxidation reaction so that spontaneous charge transfer can occur (ΔG < 0). In our case, the potential of the electrolyte must be i) above that of the solid to be able to oxidize Ni(OH)2 to NiOOH during charging and ii) below that of the solid to be able to reduce NiOOH to Ni(OH)2 during discharge. In the case of the charging process (**Figure 3a**), ferrocyanide is oxidized to ferricyanide in the electrochemical reactor. The ferricyanide in the electrolyte flows to the external reservoir. At low state of charge (point 1 ,2 and 3 in Fig 3a), the redox potential of the electrolyte is below that the solid so that spontaneous charge transfer does not take place. The potential of the electrolyte increases with increasing state of charge following Nernst behavior. At a given state of charge, the redox potential of the electrolyte is above that of the solid so that ferricyanide oxidizes $Ni(OH)_2$ to NiOOH reducing itself to ferrocyanide and returning to the electrochemical reactor in its discharged state. At this point, the redox electrolyte starts to behave as redox wire transporting charges from the electrochemical reactor to the solid material confined in the external reservoir. Once the solid active material is fully oxidized (charged), ferricyanide accumulates till the battery is fully charged. During discharging process (**Figure 3b**), the redox potential of the electrolyte is above that of the solid at high state of charge (point 1, 2 and 3 in **Figure 3b**), so that ferrocyanide cannot reduce NiOOH to Ni(OH)2. The potential of the electrolyte decreasing with the state of charge. At a given state of charge, the redox potential of the electrolyte is below that of the solid so that ferrocyanide reduces Ni(OH)2 to NiOOH oxidizing itself to ferricyanide and returning to the electrochemical reactor in its charged state. The ferrocyanide in the electrolyte flows to the external reservoir. Once the solid active material is fully reduced (discharged), ferrocyanide accumulates till the battery is fully discharged.

Evidence of Spontaneous Charge Transfer between $Fe(CN)_6^{3-}/Fe(CN)_6^{4-}$ and $Ni(OH)_2/NiOOH$. We visually demonstrate that the electrochemical reactions between the pair ferrocyanide/ferricyanide and $Ni(OH)_2$/NiOOH occur spontaneously. The differences in color between $Ni(OH)_2$ and NiOOH which are green and black, respectively,[14] allow us to observe transformations between these two phases. **Figure 4** shows photograms of two videos of the spontaneous reactions. A sample of $Ni(OH)_2$ was placed on a filter paper (**Figure 4a-c**). A solution of ferricyanide was added to sample. When ferricyanide was added, the particles changed color, from green to black (**Figure 4b**), indicating the oxidation of $Ni(OH)_2$ to NiOOH. After rinsing the sample with 1 M KOH solution, ferrocyanide was added to the black sample of NiOOH. The addition of ferrocyanide led to another change of color, from black to green (**Figure 4c**), which indicates the reduction of NiOOH back to $Ni(OH)_2$. This experiment shows that ferricyanide is able to oxidize $Ni(OH)_2$ to NiOOH, while ferrocyanide is able to reduce NiOOH to $Ni(OH)_2$. To confirm that these processes are also reversible in a flow battery, we assembled an electrochemical flow cell that contained a ferrocyanide solution. In an external reservoir, a sample of $Ni(OH)_2$ was immersed (**Figure 4d**). Ferrocyanide in the solution was electrochemically oxidized to ferricyanide in the electrochemical reactor. When the electrochemically generated ferricyanide reached the external reservoir, it oxidized the particles of $Ni(OH)_2$ to NiOOH, changing the color of the sample from green to black (**Figure 4e**). Once the first step was ended, the ferricyanide solution that was previously generated was electrochemically reduced to ferrocyanide in a second step. When the electrochemically generated ferrocyanide reached the external reservoir, it was able to reduce NiOOH to $Ni(OH)_2$, which was visualized by the change in color, from black to green (**Figure 4f**).

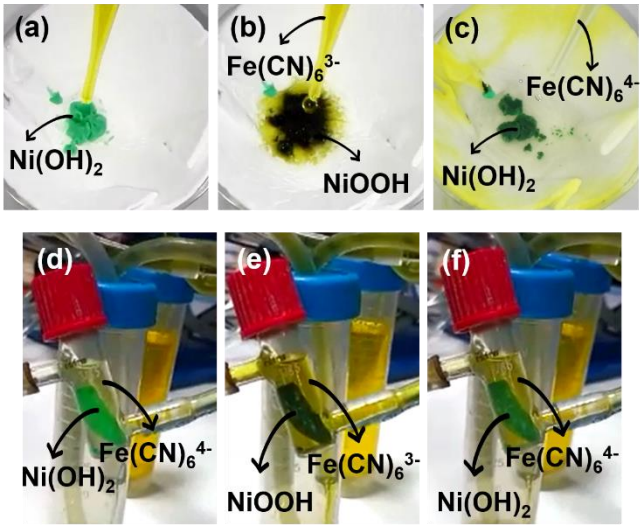

Figure 4. Photograms of two videos. Video 1: (**a**) a sample of Ni(OH)2 is placed in a paper filter, (**b**) Ferricyanide is added to the Ni(OH)2 sample, which leads to a change of the color from green to back, indicating the oxidation of $Ni(OH)_2$ to NiOOH. (**c**) Ferrocyanide is added to the sample, which provokes the reduction of NiOOH back to $Ni(OH)_2$ recovering its initial green color. Video 2: (**d**) a sample of $Ni(OH)_2$ is immersed in the external reservoir of a flow cell in the presence of ferrocyanide. (**e**) Ferrocyanide is electrochemically oxidized to ferricyanide, which reacts spontaneously with $Ni(OH)_2$ in the external reservoir generating NiOOH. The reaction is evidenced by the change of color of the sample from green to black. (**f**) Ferricyanide that was previously generated is electrochemically reduced to ferrocyanide, which reacts spontaneously with NiOOH, returning to its initial reduced state $Ni(OH)_2$.

Thermodynamics of Charge Transfer between Ferrocyanide / Ni(OH)2. It should be first noted that evaluation of the thermodynamic spontaneity and reversibility of charge transfer reaction between liquid and solid requires gathering information at equilibrium condition so that the use of cyclic voltammetry is strongly discouraged. For instance, reaction between ferrocyanide solution and Ni(OH)2 electrode appears not to be spontaneous when evaluated by cyclic voltammetry (**Fig S1** in ESI). On the other hand, evolution of the potential at open circuit with the state of charge allows for unambiguous determination of spontaneity from a thermodynamic perspective (**Figure 5**). When fully charged, the electrolyte reaches the most oxidizing potential, which is high enough to oxidize Ni(OH)2 up to its 95 % state of charge (**Figure 5a**). When fully discharged, the potential of the electrolyte is low enough to reduce NiOOH completely back to Ni(OH)2. Therefore, thermodynamically speaking, a ferrocynide solution could act as bidirectional redox wire to charge / discharge Ni(OH)2/NiOOH in a range between 0 – 95 % state of charge. Kinetics of the charge transfer reaction, contact area between solid and liquid and practical state of charge achievable for the electrolyte (at 1 % and 99 % state of charge, the concentration of reactant in the electrolyte is so low that high current densities cannot be sustained) will determine how much charge can be stored reversibly in the solid material under given conditions. For instance, when the electrolyte is limited to operate in a range of 10 % - 90 % state of charge, the oxidizing and reducing capability of the electrolyte is decreased limiting the accessible state of charge of the solid material to a range between 0 % - 85 % state of charge (**Figure 5b**).

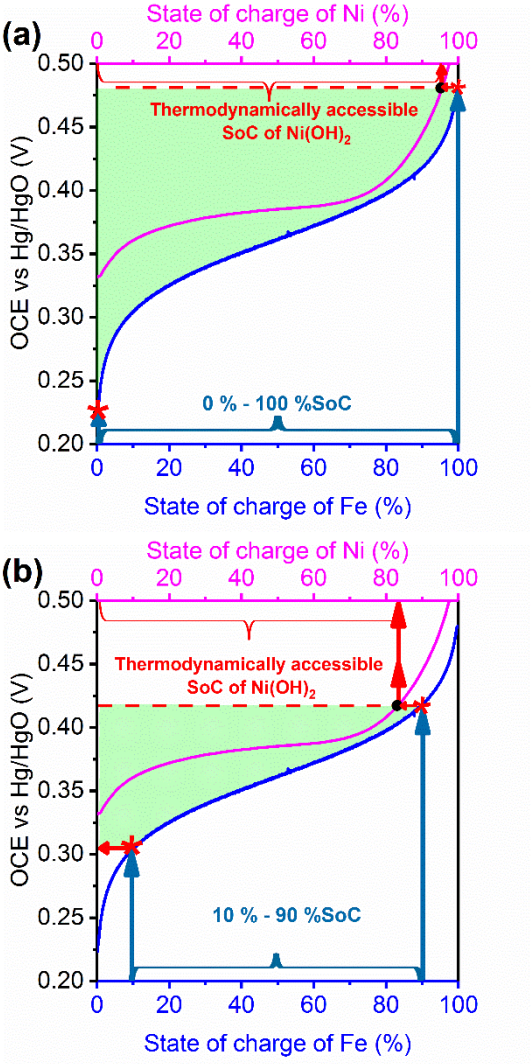

Figure 5. Evolution of potential measured at open circuit in 1 M KOH for a ferrocynide solution (blue line) and a commercial Ni(OH)2 electrode taken from a Ni-MH battery. (**a**) Full charge and discharge of the ferrrocyanide solution (0 – 100 % state of charge) allows Ni(OH)2 to be charged and dischargde between 0 – 95 % state of charge. (**b**) When ferrocynyde is charged / discharged between 10 – 90 % state of charge (more practical scenario), the Ni(OH)2 is limited to 0 – 85 % state of charge.

Influence of KOH concentration in the driving force for charge transfer reaction. An important condition for reversible charge transfer is that the redox potential of electrolyte and solid are close. In the case of potassium ferrocyanide and $Ni(OH)_2$ in KOH aqueous solution, the redox potential of ferrocyanide increases (K^+ dependent) while that of $Ni(OH)_2$ decreases (H^+ dependent), as the concentration of KOH. Hence, working conditions can be adjusted depending on the final application to increase the driving force of charge transfer during charging process or

discharging process by changing the concentration of KOH, according to Nernst law. **Figure 6** shows the evolution of the redox potential as a function of the concentration of KOH that was measured experimentally at 50 % state of charge for a ferrocyanide solution and $Ni(OH)_2$ electrode. In 1 M KOH, the potentials at 50 % overlap, which is the ideal case as illustrated above in Figure 3. Above 1 M KOH, the average potential of the electrolyte will be slightly lifted with respect to the solid material. Thus, the driving force of charge transfer reaction during charging process will be increased, in detriment of discharging process, by increasing the concentration of KOH above 1 M. This case would be of interest for applications in which faster charging than discharging is required. Likewise, the driving force for charge transfer reaction during discharging process can be increased, in detriment of charging process, by decreasing the concentration of KOH below 1 M. This case would be of interest for applications in which faster discharging than charging is required.

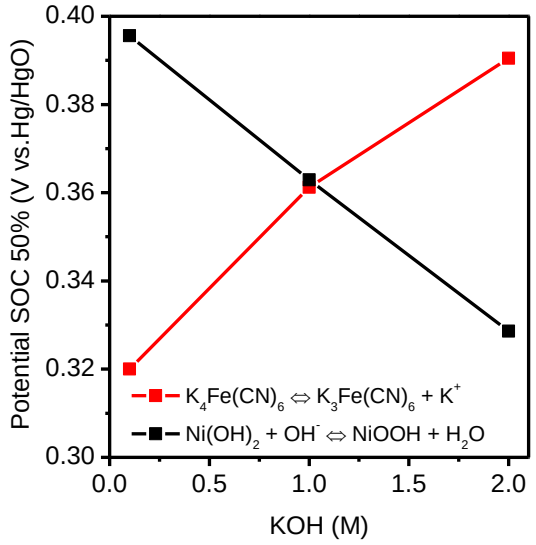

Figure 6. Evolution of redox potential measured at open circuit at 50 % state of charge with the concentration of KOH. The relation is not completely linear because the redox potential is dependent on the activity of species, instead of concentration. At high concentration, the activity coefficient diverges from the unity.

Electrochemical Quantification of Charge Storage in the Solid Material Confined in the Reservoir. Charge storage in the solid material confined in the reservoir was further demonstrated and quantified electrochemically using a symmetrical flow cell in which ferrocyanide and ferricyanide are used as active species for the positive and negative compartment, respectively (**Figure 7a**). A large excess of ferricyanide (three times the amount of ferrocyanide) was used in the negative compartment so that the positive compartment became the limiting side. This symmetrical configuration allows easy evaluation of the reactions occurring in the limiting compartment. In addition, interfering of hydrogen evolution and oxygen reduction were avoided, making this configuration very useful for fundamental studies in flow batteries.[15,16] Therefore, all values are referred to the limiting side, which initially contains ferrocyanide.

To quantify the amount of charge stored in the active solid material, we carried out a series of experiments in which the amount of charge stored in the pair ferrocyanide/ferricyanide was known as well as the mass of $Ni(OH)_2$ added to the external reservoir. We employed $Ni(OH)_2$ electrodes taken from commercial Ni-MH batteries (Panasonic HHR-110AA) due to their good performance and easy handling. The charge storage capacity of these electrodes was 125 mAh $g_{electrode}^{-1}$. Since the specific capacity of $Ni(OH)_2$ is 250 mAh $g_{Ni(OH)2}^{-1}$, $Ni(OH)_2$ accounts for *ca.* 50 % of the electrode mass. In the absence of $Ni(OH)_2$ electrode, the charge stored in the ferrocyanide/ferricyanide electrolyte solution was very close to its maximum theoretical value since an experimental value of 7.3 Ah L^{-1} was obtained for a maximum value of 8.0 Ah L^{-1} (0.3 M ferrocyanide). In the presence of $Ni(OH)_2$ electrode in the external reservoir, the reversible charge increased significantly (**Figure 7b**). Indeed, a linear relationship between the amount of $Ni(OH)_2$ added to the electrolyte and the volumetric charge capacity was obtained. At the applied current density of ±20/2 mA cm^{-2}, the utilization rate of $Ni(OH)_2$ for these three cases was ca. 40 %, which is the ratio between charge stored in $Ni(OH)_2$ and maximum possible value (Section 2 in ESI). The voltage profile (**Figure 7c**) shows two important points: i) low current densities are required to achieve volumetric capacities near 30 Ah L^{-1} and utilization rates of 40 %; and ii) different volumetric capacities are obtained at 20 mA cm^{-2} for charge (15 Ah L^{-1}) and discharge (20 Ah L^{-1}) processes, indicating that the discharge process is faster. Clearly, kinetics need to be improved by addressing material engineering aspects, e.g. particles size, as well as engineering aspects of the reservoir, e.g. distribution of electrolyte through solid active material (pieces of Ni electrode extracted from commercial NiMH batteries were immersed in the reservoir). However, these aspects do not explain the asymmetrical behavior during charge and discharge process observed in **Figure 7c**. This feature is related to an asymmetrical driving force for charge transfer reaction during charge-discharge process. The driving forces for charge and discharge process can be adjusted by the concentration of KOH. As discharge process is faster than charge process, concentrations above 1.5 M KOH appear to be feasible. However, the solubility of potassium ferrocyanide is further diminished by increasing the concentration of KOH so that 1.5 M KOH was set as upper limits. Our symmetrical cell using Ni(OH)2 shows good capacity retention upon cycling (**Figure 7d**), remaining well above the maximum theoretical value of the electrolyte (104 mAh). It should be noted that the stability of ferrocyanide in alkaline media is under debate since strong capacity fading was reported (capacity fade of 50 % in 100 cycles).[15] Figure SXX shows the cycle stability in the absence of Ni(OH)2 indicating two points: i) ferrocyanide is not as unstable as previously claimed, ii) unbalancing of the sys-

tem is likely responsible for the capacity decay since similar decay is observed with and without Ni(OH)2. On the other hand,

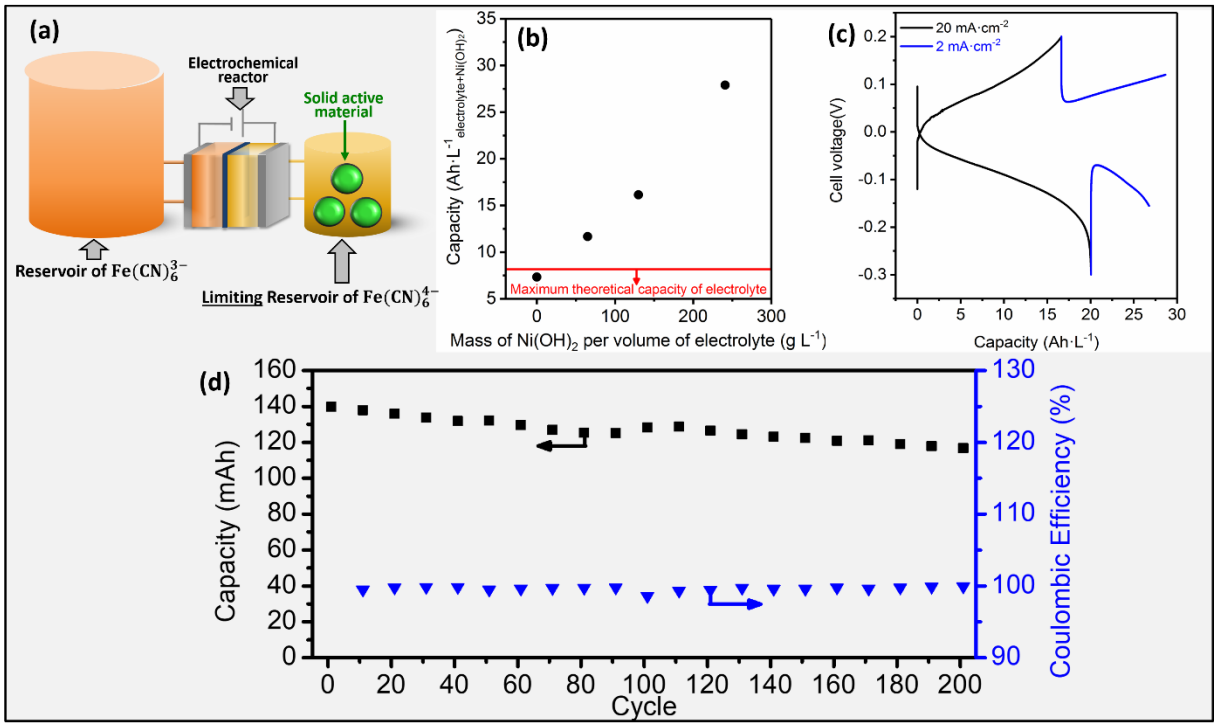

Figure 7. Electrochemical evidence of charge storage in Ni(OH)2 using a symmetrical cell. (**a**) Scheme of the symmetrical cell based on ferricyanide // ferrocyanide solutions. The volume of the reservoir containing ferricyanide was significantly larger than that containing ferrocyanide so that the latter became the limiting side. (**b**) Evolution of the reversible charge stored as a function of the mass of Ni(OH)2 added to the electrolyte (g_{solid} / $L_{electrolyte}$). The utilization rate in all cases was close to 40 % at the applied current density of ± 20 / 2 mA cm^{-2}. (**c**) Voltage profile of a cell containing 240 g of Ni(OH)2 per liter of electrolyte. (**d**) Capacity versus number of cycles at ± 20 mA cm^{-2} (maximum capacity of electrolyte of 104 mAh; 13 mL 0.3 M $K_4Fe(CN)_6$ in 1 M KOH) for XXg Ni(OH)2 per liter of electrolyte.

One disadvantage of the mixed cation mechanism (H^+ and K^+ for Ni(OH)2 and $K_4Fe(CN)_6$) is that the concentration of KOH will decrease with increasing state of charge. At very low concentration of KOH, ferrocyanide might not be able to act as redox mediator (Figure 6). The maximum volumetric capacity can be estimated by determining the range of KOH concentration for which the concept works. In our case, we know the it works between 1.5 M (Figure 7) and 0.5 M KOH (**Fig. S2** in ESI). For a targeted system with 60 Ah L^{-1} for each positive and negative compartment (e.g. phenazine), changes in KOH concentration between 1.5 M and 0.5 M give rise to 2 M variation (1 M from each compartment). Under these conditions, the positive compartment should be able to deliver 63.6 Ah L^{-1}: 2 M x 26.8 Ah L^{-1} (Faraday constant) + 10 Ah L^{-1} (ferrocyaide solution). Therefore, practical values of energy densities > 40 Wh L^{-1} are achievable by the addition of relatively low amount of Ni(OH)2.

Implementation in Full Alkaline Flow Batteries. The highest practical value of energy density (*ca.* 9 Wh L^{-1}) for an alkaline flow battery was realized by Wei et al. using a phenazine derivative // $K_4Fe(CN)_6$. The volumetric charge storage capacities of negative and positive compartment realized was 67 Ah $L^{-1}_{anolyte}$ and 7 Ah $L^{-1}_{catholyte}$, respectively, making the positive compartment the bottleneck in terms of energy density. Therefore, we implemented the concept in this battery chemistry. **Figure 8a** shows the voltage profile for a 7,8-dihydroxyphenazine-2-sulfonic acid (0.5 M eq.) // $K_4Fe(CN)_6$ (0.3 M) flow battery for three scenarios: a1) limited by $K_4Fe(CN)_6$ (10 mL, *80 mAh of ferrocyanide* and 10 mL, *130 mAh of phenazine*) a2) limited by phenazine (20 mL, *160 mAh of ferrocyanide* and 10 mL, *130 mAh of phenazine*) and a3) limited by $K_4Fe(CN)_6$ (10 mL, *80 mAh of ferrocyanide* and 10 mL, *130 mAh of phenazine*) in the presence of $Ni(OH)_2$. Despite the charge in scenario a3 was supposed to be limited to 80 mAh by the amount of $K_4Fe(CN)_6$ (80 mAh of ferrocyanide and 130 mAh of phenazine), the addition of $Ni(OH)_2$ in the positive reservoir enabled this cell to store 120 mAh, which is the maximum practical capacity of phenazine. Hence, solid $Ni(OH)_2$ confined in the reservoir stores additional charges in the positive compartment while occupying little volume. **Figure 8b** shows that the volumetric capacity of the positive compartment increased from 8 Ah $L^{-1}_{catholyte}$ to 13 Ah $L^{-1}_{catholyte+Ni(OH)2}$, when 150 $g_{Ni(OH)2}$ $L^{-1}_{catholyte}$ was added, which accounts for 14 % utilization of the theoretical charge storage capacity of the added $Ni(OH)_2$. A capacity decay was observed during the first cycles. Since the capacity in symetrical cell was did not show this behavior,

the decay is ascribed to the negative compartment likely to O2 reduction due to the absence of Ar-filled glovebox (Figure 7d). In cycle 50, the cuttof was lifted so that more Ni(OH)2 was used to balance the cell, and the value stabilized around 12 Ah $L^{-1}_{catholyte+Ni(OH)2}$. Taking the value after 100 cycles (150 hours) an average capacity retention of 99.92 % per cycle and 98.72 % per day is obtained. It should be noted that similar capacities retention values were obtained previously for phenazine // $K_4Fe(CN)_6$ in Ar-filled glovebox, which was attributed to a unimolecular decay mechanism,[9] and could also attributed to the decay in our case. The efficiencies over 100 cycles are shown in **Fig. S3** in ESI, remaining stable at >99% and >80 % for coulombic and voltage efficiency, respectively.

To achieve higher energy density, the concentration of phenazine was increased from 0.5 M eq. (0.25 M and two-electron reaction) to 2 M eq. (1 M and two-electron reaction). **Figure 8c** shows the voltage profile for a phenazine (2 M eq.) // $K_4Fe(CN)_6$ (0.3 M) flow battery in the absence and presence of $Ni(OH)_2$. Since the volumetric capacity of phenazine is considerably larger than that of $K_4Fe(CN)_6$, a large volume of catholyte was required in the absence of $Ni(OH)_2$ leading to lower total volumetric capacity (catholyte+anolyte). In the presence of $Ni(OH)_2$, the required volume of catholyte is lower since $Ni(OH)_2$ stores additional charges resulting in higher total volumetric capacity (catholyte+$Ni(OH)_2$+anolyte). The resulting energy density was 16 Wh L^{-1}_{total} (18 % utilization rate of $Ni(OH)_2$) which represents a clear step forward for alkaline flow batteries in terms of the energy density (**Figure 8d**).

The versatility of this concept was demonstrated by implementing it in other 2 alkaline flow batteries: anthraquinone // $K_4Fe(CN)_6$ flow battery and Zn // $K_4Fe(CN)_6$ hybrid-flow battery (**Fig. S4** and **S5** in ESI). In both cases, the volumetric charge storage capacity of the positive compartment was significantly increased from 7.8 Ah $L^{-1}_{catholyte}$ in absence of $Ni(OH)_2$ to 11 – 13 Ah $L^{-1}_{catholyte}$ in the presence of $Ni(OH)_2$ (utilization rate of $Ni(OH)_2$ of 14 – 22 %).

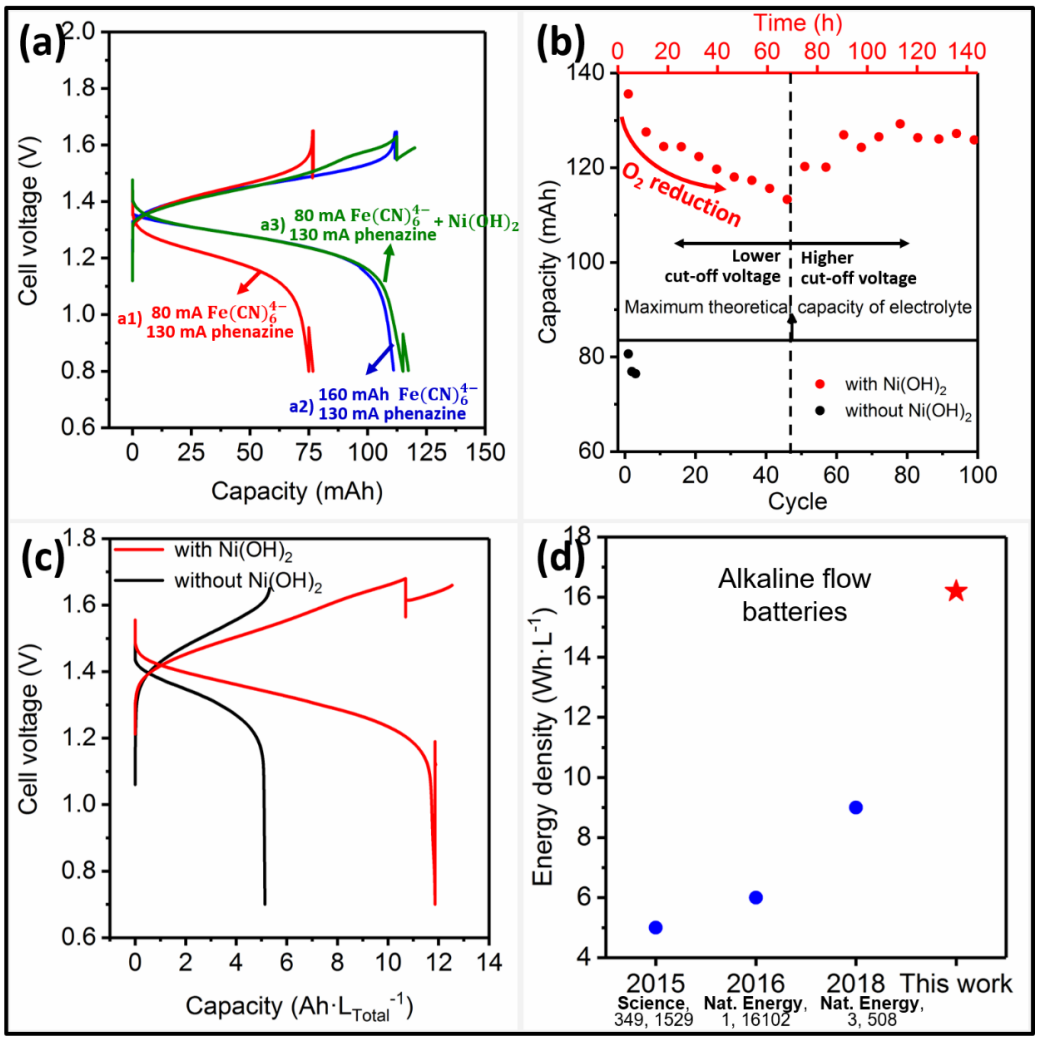

Figure 8. Electrochemical performance of a phenazine derivative // K4Fe(CN)6 – Ni(OH)2. (**a**) Voltage profiles for three scenarios: a1) limited by K4Fe(CN)6 (10 mL 0.3 M K4Fe(CN)6 and 10 mL 0.5 M eq. phenazine), a2) limited by phenazine (20 mL 0.3 M K4Fe(CN)6 and 10 mL 0.5 M eq. phenazine) and a3) addition of 1.5 g of Ni(OH)2 to conditions of a1 (10 mL 0.3 M K4Fe(CN)6 and 10 mL 0.5 M eq. phenazine). (**b**) Charge capacity over 100 cycles $g_{(Ni(OH)2)}$ $\mathbf{L^{-1}_{catholyte}}$ were added (10 mL 0.3 M K4Fe(CN)6, 1.5 g Ni(OH)2 and 10 mL 0.5 M eq. phenazine). (**c**) Voltage profile in absence (100 mL 0.3 M K4Fe(CN)6, and 12 mL 2 M eq. phenazine)

and presence of Ni(OH)2 (25 mL 0.3 M K4Fe(CN)6, 5.9 g Ni(OH)2 and 12 mL 2 M eq. phenazine). (**d**) State-of-the-art energy density demonstrated for an alkaline flow battery (our value was obtained from (c)). The utilization rates varied between 14 and 18 % at the applied current density of ± 20 / 2 mA cm-2. Note that the lower current density was not necessary in many cases due to the longer charge / discharge time compared to other experiments.

Trade-off for utilization rate of Ni(OH)2. The use of solid $Ni(OH)_2$ materials in flow batteries may raise some concerns regarding cycle life and cost. However, I) $Ni(OH)_2$ – MH batteries have demonstrated a cycle life of 20.000 – 300.000 cycles for a depth of charge of 50 – 10 %, respectively,[17] which would result in an increase in energy density of 220 % – 50 % for a phenazine – $K_4Fe(CN)_6$ flow battery for a the concentration of $Ni(OH)_2$ in the reservoir of 250 $g_{Ni(OH)2}$ $L^{-1}_{catholyte}$ (**Fig. S7** in ESI). II) In contrast with vanadium, nickel is not considered to be a critical/strategic material by the US government and EU commission and its price is almost 10-fold lower than that of vanadium (35 USD kg^{-1} and 3.8 USD kg^{-1} for vanadium pentoxide and nickel sulfate, respectively).[18,19] Since there is no estimated cost of the phenazine derivative, the impact of adding $Ni(OH)_2$ was calculated for the chemical cost (electrolyte + $Ni(OH)_2$) of an anthraquinone – $K_4Fe(CN)_6$ flow battery (Fig S5 in ESI). This analysis revealed that the chemical cost strongly depends on the utilization rate of $Ni(OH)_2$: the higher the utilization rate, the lower the chemical cost. For a utilization rate of 40 %, addition of $Ni(OH)_2$ does not affect the chemical cost. Below and above this value, the presence of $Ni(OH)_2$ increases and decreases, respectively, the chemical cost. In terms of energy density (**Fig. S6** in ESI), since the volumetric capacity might be limited to ca. 60 Ah L^{-1} (ca. 40 Wh l^{-1}), further optimization of this concept should target utilization rates of 30 % -40 % as compromised between cost and cyclibility, and amount of Ni(OH)2 per liter of electrolyte of 250 - 350 g ml^{-1} to achieve 40 Wh L^{-1}(**Fig S7** in ESI). Obviously, further improvement at system level will be required to reach those values.
The case of Zn – K4Fe(CN)6-Ni(OH) is different since OH^- /H^+ are the ions involved in the Zn/ZnO reaction leading to a rocking chair mechanism for the full system in which the concentration of KOH would not change. Therefore, the theoretical energy density of this systems is not limited to 40 Wh L-1, and should be the chemistry of choice for applications that require higher values of energy density.
Finally, it should also be noted that solid $Ni(OH)_2$ can be easily collected from the reservoirs strongly facilitating its recycling, which would bring additional economic and environmental benefits.

CONCLUSION

The energy density of the family of ferrocyanide-based alkaline flow batteries is significantly increased by the strategy presented here: potassium ferrocyanide acts not only as dissolved electroactive species, but also as charge carrier to store energy in a solid active material located in the external positive reservoir. Kinetics of charge transfer reaction between liquid and solid as well as cell design are two critical aspects that still need to be improved for optimal operation and maximum performance. This strategy is generally valid for any alkaline flow batteries based on the use of ferrocyanide ion in the positive compartment. The concept is implemented for two alkaline flow systems: antraquinone – $K_4Fe(CN)_6$ and phenazine derivative – $K_4Fe(CN)_6$. For the latter, an energy density of 16 Wh L^{-1}_{total} and a capacity retention of 99.92 % per cycle and 98.72 % per day during 100 cycles were demonstrated.
The versatility of the concept was demonstrated by implementing it in three battery chemistries: Zn – $K_4Fe(CN)_6$, anthraquinone – $K_4Fe(CN)_6$ and phenazine – $K_4Fe(CN)_6$. Therefore, it is likely that this concept will be valid for new alkaline chemistries that can be developed in the near future.

EXPERIMENTAL SECTION

Materials. All chemicals were purchased from Sigma Aldrich and used as received. 2,6-dihydroxyanthraquinone (2,6-DHAQ) (≥95% purity) from Glentham Life Science was recrystallized by solving it in DMF and subsequently making the purer solids precipitates by adding water. Vacuum filtration was used for crystals isolation.
Synthesis of nickel hydroxide. Nickel hydroxide for optical demonstration of reversible charge storage (Figure 4) was prepared from nickel chloride. Nickel chloride (12 g) was added to 25 mL of 2 M KOH solution and stirred at room temperature during 1h. Then, 2 M KOH was added till complete 100 mL of solution. After 1 h, the desired product was collected by vacuum filtration, washed with distilled water and dried at 40 ºC overnight.
Nickel hydroxide for electrochemical measurements (Figure 5 and 6) was taken from commercial NiMH batteries (Panasonic HHR-110AA). The battery was disassembled and the electrode was directly extracted. The charge storage capacity of Ni electrodes was 125 mAh $g^{-1}_{electrode}$. Since the specific capacity of $Ni(OH)_2$ is 250 mAh $g^{-1}_{Ni(OH)2}$, $Ni(OH)_2$ accounts for *ca.* 50 % of the electrode mass.

Synthesis of 7,8-dihydroxyphenazine-2-sulfonic acid. 7,8-dihydroxyphenazine-2-sulfonic acid was prepared by following the described procedure previously reported.[9] The isolated compound showed identical spectroscopic data as those reported therein (**Fig. S8** and **Fig S9** in ESI).

Preparation of electrolytes. In the symmetric flow cell, the catholyte was prepared by dissolving potassium ferrocyanide (3.8 g) in 1.5 M KOH to afford 30 mL 0.3 M ferrocyanide. The anolyte was prepared by dissolving potassium ferrocyanide (7.9 g) and potassium ferricyanide (5.07 g) in 1.5 M KOH to afford 120 mL 0.1 M ferrocyanide, 0.2 M ferricyanide. The large excess of ferricyanide in the anolyte ensured that the catholyte was the limiting side (24 mmol versus 9 mmol).
In the phenazine // $K_4Fe(CN)_6$ flow cell, the same method was used for preparing catholyte. The anolyte was pre-

pared by dissolving either 0.9 g of 7,8-dihydroxyphenazine-2-sulfonic acid in 1.9 M KOH to afford 10 mL 0.3 M phenazine and 1 M KOH; or 3.6 g of 7,8-dihydroxyphenazine-2-sulfonic acid in 4 M KOH to afford 12 mL 1 M phenazine (2 M eq. considering the exchange of 2 electrons) and 1 M KOH.

In the Zn // $K_4Fe(CN)_6$ hybrid-flow cell, the same method was used for preparing catholyte. The anolyte was prepared by dissolving zinc oxide (0.5 g) in 2 M KOH to afford 13mL 0.5 M ZnO and 1 M KOH.

In the anthraquinone // $K_4Fe(CN)_6$ flow cell, the catholyte was prepared by dissolving potassium ferrocyanide (3.8 g) in 1.5 M KOH to afford 30 mL 0.3 M ferrocyanide. The anolyte was prepared by dissolving potassium 2,6-DHAQ (2.1 g) in 2.1 M KOH to afford 30 mL 0.3 M 2,6-DHAQ and 1.5 M KOH.

Deionized water was used to prepare the electrolytes and 2,6-DHAQ and ferrocyanide were purged with nitrogen prior to use.

Flow Batteries. Filter-pressed flow cell using Nafion 212 and graphite felt as the ion selective membrane and electrodes were used in this study. The projected area of the cell was 24 cm^2 in the case of symmetrical cell and anthraquinone // $K_4Fe(CN)_6$ flow battery, and 9 cm^2 for phenazine derivative // $K_4Fe(CN)_6$ flow battery. A modified filter-pressed flow cell of 9 cm^2 of projected area was used for Zn // $K_4Fe(CN)_6$. The flow rate was fixed at *ca*. 50 mL min^{-1}

Electrochemical characterization. Galvanostatic charge-discharge measurements were conducted using a Biologic VMP multichannel potentiostat. The battery was galvanostatically charged at 20 $mAcm^{-2}$ and 2 $mAcm^{-2}$ with voltage limits of 1.37 and 1.33 V respectively. Subsequently, it was discharge at current densities between -20 and -2 $mAcm^{-2}$ with voltage limit of 0.5 V. The upper limits were adjusted for the different chemistries: 1.37 and 1.33 V for anthraquinone, 1.68 and 1.64 V for phenazine and 2 V for Zn.

ASSOCIATED CONTENT

Supporting Information. Discussion on thermodynamics for reversible charge transfer reaction. Calculation of volumetric charge storage capacity of Ni-based batteries and utilization rate of $Ni(OH)_2$ Implementation of proposed concept in Anthraquinone // $K_4Fe(CN)_6$–$Ni(OH)_2$ flow battery. Implementation of proposed concept in Zn // $K_4Fe(CN)_6$–$Ni(OH)_2$ hybrid-flow battery. Estimations of the impact of using $Ni(OH)_2$ in the cost of electrolyte for an anthraquinone – ferrocyanide flow battery Estimation of the impact of using $Ni(OH)_2$ in the energy density for a phenazine – ferrocyanide flow battery. Synthesis and characterization of 7,8-dihydroxyphenazine-2-sulfonic acid "This material is available free of charge via the Internet at http://pubs.acs.org.".

AUTHOR INFORMATION

Corresponding Author

* edgar.ventosa@imdea.org

Present Addresses

†If an author's address is different than the one given in the affiliation line, this information may be included here.

Author Contributions

The manuscript was written through contributions of all authors. / All authors have given approval to the final version of the manuscript.

Funding Sources

Financial support from Comunidad de Madrid in the framework of the talent attraction programme (2017-T1/AMB-5190) is gratefully acknowledged. A. M.-C. thanks Ministerio de Ciencia, Innovación y Universidades for a Ramon y Cajal contract and funding (RYC-2017-22700).

REFERENCES

(1) Soloveichik, G. L. Flow Batteries : Current Status and Trends. 2014. https://doi.org/10.1021/cr500720t.

(2) Lin, K.; Chen, Q.; Gerhardt, M. R.; Tong, L.; Kim, S. B.; Eisenach, L.; Valle, A. W.; Hardee, D.; Gordon, R. G.; Aziz, M. J.; et al. Alkaline Quinone Flow Battery. *Science (80-.).* **2015**, *349* (6255), 1529–1532. https://doi.org/10.1126/science.aab3033.

(3) Noack, J.; Roznyatovskaya, N.; Herr, T.; Fischer, P. The Chemistry of Redox-Flow Batteries. *Angew. Chemie Int. Ed.* **2015**, *54* (34), 9776–9809. https://doi.org/10.1002/anie.201410823.

(4) Ding, C.; Zhang, H.; Li, X.; Liu, T.; Xing, F. Vanadium Flow Battery for Energy Storage: Prospects and Challenges. *J. Phys. Chem. Lett.* **2013**, *4* (8), 1281–1294. https://doi.org/10.1021/jz4001032.

(5) Final List of Critical Minerals 2018.

(6) The 2017 list of Critical Raw Materials for the EU.

(7) Orita, A.; Verde, M. G.; Sakai, M.; Meng, Y. S. A Biomimetic Redox Flow Battery Based on Flavin Mononucleotide. *Nat. Commun.* **2016**, *7* (1), 13230. https://doi.org/10.1038/ncomms13230.

(8) Lin, K.; Gómez-Bombarelli, R.; Beh, E. S.; Tong, L.; Chen, Q.; Valle, A.; Aspuru-Guzik, A.; Aziz, M. J.; Gordon, R. G. A Redox-Flow Battery with an Alloxazine-Based Organic Electrolyte. *Nat. Energy* **2016**, *1* (9), 1–8. https://doi.org/10.1038/nenergy.2016.102.

(9) Hollas, A.; Wei, X.; Murugesan, V.; Nie, Z.; Li, B.; Reed, D.; Liu, J.; Sprenkle, V.; Wang, W. A Biomimetic High-Capacity Phenazine-Based Anolyte for Aqueous Organic Redox Flow Batteries. *Nat. Energy* **2018**, *3* (6), 508–514. https://doi.org/10.1038/s41560-018-0167-3.

(10) Seventeenth report of the joint FAO-WHO Expert Committee on Food Additives (1974).

World Health Organ. Tech. Rep. Ser. 539, 1–40. Toxicological Evaluation of Certain Food Additives with a Review of General Principles and of Specifications. Seventeenth.

(11) Luo, J.; Hu, B.; Debruler, C.; Bi, Y.; Zhao, Y.; Yuan, B.; Hu, M.; Wu, W.; Liu, T. L. Unprecedented Capacity and Stability of Ammonium Ferrocyanide Catholyte in PH Neutral Aqueous Redox Flow Batteries. *Joule* **2019**, *3* (1), 149–163. https://doi.org/10.1016/j.joule.2018.10.010.

(12) Zhou, M.; Huang, Q.; Pham Truong, T. N.; Ghilane, J.; Zhu, Y. G.; Jia, C.; Yan, R.; Fan, L.; Randriamahazaka, H.; Wang, Q. Nernstian-Potential-Driven Redox-Targeting Reactions of Battery Materials. *Chem* **2017**, *3* (6), 1036–1049. https://doi.org/10.1016/J.CHEMPR.2017.10.003.

(13) Yu, J.; Fan, L.; Yan, R.; Zhou, M.; Wang, Q. Redox Targeting-Based Aqueous Redox Flow Lithium Battery. *ACS Energy Lett.* **2018**, *3* (10), 2314–2320. https://doi.org/10.1021/acsenergylett.8b01420.

(14) Carpenter, M. K.; Conell, R. S.; Corrigan, D. A. The Electrochromic Properties of Hydrous Nickel Oxide. *Sol. Energy Mater.* **1987**, *16* (4), 333–346. https://doi.org/10.1016/0165-1633(87)90082-7.

(15) Luo, J.; Sam, A.; Hu, B.; DeBruler, C.; Wei, X.; Wang, W.; Liu, T. L. Unraveling PH Dependent Cycling Stability of Ferricyanide/Ferrocyanide in Redox Flow Batteries. *Nano Energy* **2017**, *42*, 215–221. https://doi.org/10.1016/J.NANOEN.2017.10.057.

(16) Goulet, M.-A.; Aziz, M. J. Flow Battery Molecular Reactant Stability Determined by Symmetric Cell Cycling Methods. *J. Electrochem. Soc.* **2018**, *165* (7), A1466–A1477. https://doi.org/10.1149/2.0891807jes.

(17) Brady, M. Assessment of Battery Technology for Rail Propulsion Application. *United States. Fed. Railr. Adm.* **2017**, https://rosap.ntl.bts.gov/view/dot/35526.

(18) Www.Vanadiumprice.Com Accessed 27/03/2019.

(19) Www.Price.Metal.Com Accessed 27/03/2019.

SYNOPSIS TOC

Mediated alkaline flow batteries: from fundamentals to application